Romanian Journal of Mechanics
Volume 5, Issue 2/2020, pp.51-60, ISSN 2537 - 5229, rjm.journals.smta.ro

NONLINEAR OSCILLATIONS IN METALLIC BILAYERS FILMS

Iulian **GIRIP**[1], Călin **CHIROIU**[2]

[1] Institute of Solid Mechanics Romanian Academy
[2]Torino, Italy

Corresponding author: Iulian GIRIP, E-mail: iuliangirip@gmail.com

Abstract The paper is concerned with the oscillations with small amplitude in initially deformed elastic metallic bilayers. The variation of sound speeds with initial strain and the measured magnitude of the acousto-elastic effect are used to determine the biaxial modulus and the elastic constants for a deformation in the [111] direction.

Key words: Bilayers films, constitutive law, biaxial modulus, supermodulus.

1. INTRODUCTION

The foils of metallic bilayers films (Au/Ni, Cu/Pd, etc.) contain short-wavelength 1D composition modulations due to the vapor deposition and the strong preferred orientation of [111] normal to the plane of the foil [1]. The increase in elastic modulus has been measured experimentally in Au/Ni and Cu/Pd metallic multilayer structures [2-4]. It is observed in these multilayers that the measured biaxial modulus was two to three times larger than the value predicted by the simple rule of mixture. For example, a composition-modulated Cu-Ni foil of 66% Cu has a reported Y[100] value of 0.23 TPa. This value is over 50% greater than that of a bulk Cu-Ni alloy of the same Cu composition (Y[100]=0.14 TPa). Similar results have been reported for Au-Ni, Cu-Pd and Ag-Pd composition modulated foils [5-7]. All the models start with the implicit assumption that the effect must be associated with the fact that, for repeat distances of around 20 A, a large volume fraction of the two different metal atoms lie at or near an interface.

Conclusive examples in this regard are the chalcogenide structures which combine the Group VI elements of the Periodic Table, especially the sulfur, selenium, and tellurium compounds [8, 9].

Chalcogenide is a material which contain at least one chalcogen anion (S^{2-}) and an electropositive element (Cd^{2+}, Zn^{2+}). These materials transmit longer wavelengths in the infrared region (IR) than fluoride glasses and silica and fully meet the requirements of high level (> 96%) of the transmission index in the visible, in the near-infrared as well as in the mid-infrared spectral ranges.

The chalcogenides deposited on both sides of a surface in the fused silica (quartz), silicon (Si), germanium (Ge), calcium fluoride (CaF_2) and zinc sulfide (ZnS) have a large spectral range from 0.6μm to 20μm with a high transmission ratio of over 90% [10,11].

The enhancement of the elastic modulus of a material is known in the literature as the supermodulus effect. Since its discovery, different models have been proposed to explain, on the atomic scale, the origin of the supermodulus effect [4].

The works in the current literature assume that the increase in the biaxial modulus is the result of the interaction of the Fermi surface with the Brillouin zone, arising from the layered structure of the materials.

At a coherent interface, the component with the larger lattice constant is compressed laterally, whereas the component with the smaller lattice constant is expanded. This state of affairs produces coherence strains at the interface and the multilayer system minimizes its total energy by adjusting its interlayer spacing perpendicular to the interface plane.

In this paper we consider a multilayered binary system with *N* atomic planes per layer (i. e. A/B multilayer with AAAA…ABBB...BAAA…ABBA…arrangement of atomic planes). 1D composition modulation has a sinusoidal form. The initial crystal in its initial nondeformed state is cubic and after the initial biaxial deformation in the direction [111], it becomes orthorhombic [12-16].

The gole of this paper is to determine the elastic constants of the foil (nine elastic constants) by using ultrasonic waves transmitted through a plate-shaped sample immersed in water.

It is shown how the variation of speeds with initial strain can be used to determine these constants. The acousto-elastic effect provides wave velocities are sufficiently sensitive to the parameters to be identified, especially with the initial strain.

2. BIAXIAL DEFORMATION IN THE DIRECTION [111]

A FCC crystal cell which is biaxial deformed in the [111] direction is considered. The motion of small amplitude waves generates in this deformed crystal an infinitesimal deformation state. The effect of the initial deformations upon the elastic constants, is analysed on the base of the theory of small, infinitesimal elastic deformations superimposed on a finite elastic deformation [14-17].

Four distinct configurations of the material points relative to the origin O are introduced.

:

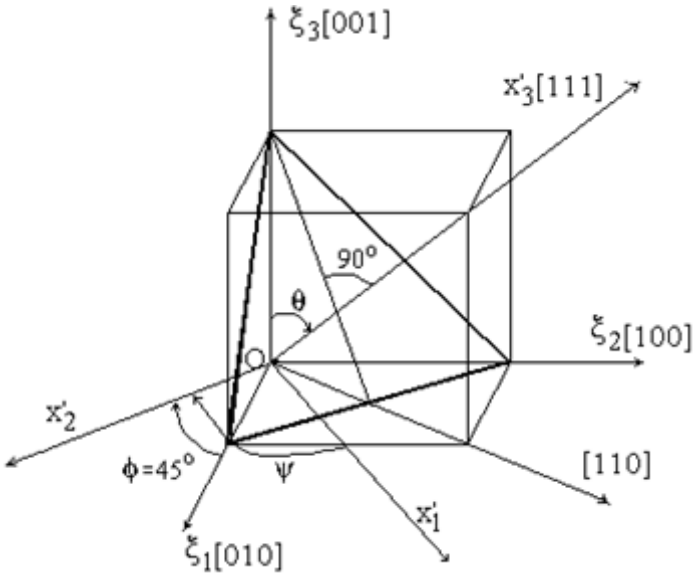

Fig.1. Representation of the set of axes (ξ_1, ξ_2, ξ_3) and (x_1', x_2', x_3').

The first system configuration is the natural or stress-free configuration C_0 represented by the crystallographic axes system $(\xi)=(\xi_1, \xi_2, \xi_3)$ shown in Fig.1. In this system, the classical definition of the elastic constants can be applied. The initial underformed material is a cubic one. The biaxial deformation of the body is carrying the configuration C_0 to an initially deformed equilibrium configuration $\tilde{C}$. In this configuration, the foil has a well textured structure.

The second system of coordinates is a geometrical system $(x') = Ox_1'x_2'x_3'$ that exploits the

geometric symmetry of the body and the symmetry of the stress state. The axis x_3' is parallel to the texture direction [111]. The orientation of the axes x_1', x_2' (usually randomly oriented in the plane of the foil perpendicularly on the texture direction) is determined by the angle ψ. The transformation from (ξ) to (x') is given by

$$x_i' = R_{ik}\xi_k \tag{1}$$

where R_{ij} is the rotation matrix. The geometrical elastic constants C'_{ijkl} in (x') are related to the primary elastic constants C^0_{ijk} in (ξ) by

$$C'_{ijkl} = R_{ip}R_{jq}R_{kr}R_{ls}C^0_{pqrs} \tag{2}$$

The material consists of two crystallites having a common texture axis $(O\,x_3')$ but which are randomly oriented on the plane (x_1', x_2') defined by other two axes. For this we use the average elastic constants for [111] texture in the cubic materials [5].

By renotting the constants α_{ijkl} by C'_{ijkl}, we obtain

$$\begin{aligned}
&C'_{11} = C'_{22} = \alpha_{11} = \alpha_{22} = (c^0_{11} + c^0_{12} + 2c^0_{44})/2\\
&C'_{33} = \alpha_{33} = (c^0_{11} + 2c^0_{12} + 4c^0_{44})/3\\
&C'_{12} = \alpha_{12} = \alpha_{21} = (c^0_{11} + 5c^0_{12} - 2c^0_{44})/6\\
&C'_{13} = C'_{23} = \alpha_{23} = \alpha_{32} = \alpha_{13} = \alpha_{31} =\\
&\qquad (c^0_{11} + 2c^0_{12} - 2c^0_{44})/3\\
&C'_{44} = C'_{55} = \alpha_{44} = \alpha_{55} = (c^0_{11} - c^0_{12} + c^0_{44})/3\\
&C'_{66} = \alpha_{66} = (c^0_{11} - c^0_{12} + 4c^0_{44})/6 = \frac{1}{2}(C'_{11} - C'_{12})
\end{aligned} \tag{3}$$

The tensor $C' = \alpha$ is composed by five independent elements, expressed as a combination of the elastic constants $C^0_{11}, C^0_{12}, C^0_{44}$. We add that the directions in (x_1', x_2') are equivalent. In this way, the material has a transversely isotropic symmetry in the foil geometrical system.

The third system of coordinates is the initially deformed equilibrium configuration $\tilde{C}$ ($X = (X_1, X_2, X_3)$). The systems (x') and (X) are related by the transformation

$$X_i = x_i'(1 + \varepsilon_i)\ , i = 1,2,3 \tag{4}$$

where ε_i are the biaxial strains

$$\varepsilon_1 = \varepsilon_2 = \varepsilon\ ,\ \varepsilon_3 = -2\frac{C'_{13}}{C'_{33}}\varepsilon\ ,\ \varepsilon_4 = \varepsilon_5 = \varepsilon_6 = 0 \tag{5}$$

The biaxial stresses are

$$\sigma_1 = \sigma_2 = \sigma,\ \sigma_3 = \sigma_4 = \sigma_5 = \sigma_6 = 0 \tag{6}$$

The relation between ε_3 and ε is obtained from the condition $\sigma_3 = 0$. The relation between the C'_{ijkl} and $\tilde{C}_{ijkl}$ are given by

$$\tilde{C}_{ijkl} = \left(\frac{\boldsymbol{X}}{\xi}\right)^{-1} \frac{\partial X_i}{\partial \xi_\mu} \frac{\partial X_j}{\partial \xi_\rho} \frac{\partial X_k}{\partial \xi_\nu} \frac{\partial X_l}{\partial \xi_\varsigma} C'_{\mu\rho\nu\varsigma} \tag{7}$$

The motion equations are

$$(\tilde{A}_{iMkN} u_{k,N})_{,M} = \tilde{\rho} \frac{\partial^2 u_i}{\partial t^2} \tag{8}$$

$$\tilde{A}_{iMkN} = \tilde{C}_{iMkN} + \tilde{t}_{MN} g_{ik} \tag{9}$$

with the initial stress $\tilde{t}_{MN}$ given by

$$\begin{aligned} &\tilde{t}_{11} = \tilde{t}_{22} = \sigma \quad , \quad \tilde{t}_{33} = 0 \\ &\tilde{t}_{ij} = 0 \quad for \quad i \neq j \end{aligned} \tag{10}$$

The system loses the transversely symmetry and becomes orthorhombic with nine constants. These constants depend on the initial state of strain and stress.

To determine the elastic constants, we need to know the constitutive law of the material, i. e. the stress-strain relation $\sigma = F(\varepsilon, \lambda, A)$, where λ and A are the wavelength and the amplitude of the modulation.

The fourth system of coordinates is the present configuration $Ox_1x_2x_3$ which is obtained from the system (X) by

$$x_i(\boldsymbol{X}, t) = X_i + u_i(\boldsymbol{X}, t) \tag{11}$$

where each component of the gradient $\frac{\partial u_i}{\partial X_j}$ of the displacement u_i of the present configuration relative to the initial configuration is small $\frac{\partial u_i}{\partial X_j} << 1$ for all times $t \geq \tilde{t}$. In other words, we assume that both the rotations and strains of the present configuration measured relative to the initial configuration remain small for all time after the initial configuration of the material points has been achieved.

3. THE NONLOCAL CONSTITUTIVE LAW

Consider that the composition of the foil and the modulation law, the elastic constants and the constitutive law of the foil are known. Therefore, the phase velocities and directions of wave motion in terms on the initial stress σ can be evaluated. This represents the direct approach. The constitutive law is needed to be known [18-20].

Let us consider the foil is composed from 2N layers, each layer having *m* atomic planes. Thus, the thickness of the foils is $h = N\lambda$. The aim of this section is to determine the stress-strain relation

$$\sigma = F(\varepsilon, \lambda, A) \tag{12}$$

where λ and A are respectively the wavelenght and the amplitude of the foil modulation, using a nonlocal theory. The hypothesis in the nonlinear theory [18-20] is that the stress at a point on the interface is not a function of the smoothed homogenized stress field at the same point but a function of the strain distribution over a certain characteristic volume centered at that point, the size of which

is the characteristic length l

$$\sigma = F(\bar{\varepsilon}(z))$$
$$\bar{\varepsilon}(z) = \frac{1}{l}[u(z+\frac{l}{2}) - u(z-\frac{l}{2})] = \frac{1}{l}\int_{-l/2}^{l/2}\varepsilon(z+s)ds \tag{13}$$

where $z \equiv X_3$ represents the modulation direction. So, we define the mean strain as a certain averaging integral over the characteristic volume V

$$\bar{\varepsilon} = \frac{1}{V}\int_V \varepsilon(x')dV \tag{14}$$

with V a sphere of radius $l/2$ centered in a point on the interface. We suppose the modulation law is $A\sin\frac{2\pi z}{\lambda}$. The condition of coherency [3,4] at the interface establishes that, at this location, layers A and B have the same in-plane lattice spacing. Away from the interface where the strain is maximum, the structure relaxes towards its unstrained condition.

The layers are bounded by interfaces, and therefore, the location of minimum strain is at the layer center. The layer under interfacial compression is bowing outward at the layer center, whereas the adjoining layer under interfacial tension bows inward at its layer center. We suppose that the term to describe the range of stress relaxation with distance from the interface is l ($\lambda = 4l$) which represents the length over the atomic planes over which the originating stress vanishes. In general a larger value of l distinguishes stiff materials from those which are compliant. The functional variation between the interfacial strain ε with z will be assumed as

$$\varepsilon_i(z) = \varepsilon_{i0}(1+\cos(\frac{4\pi z}{\lambda})),\ \varepsilon_i(z+\lambda) = \varepsilon_i(z), \tag{15}$$

i =1,2…6 , where ε_{i0} is the maximum value of strain. From (3.3) we obtain the relation

$$\bar{\varepsilon}_i = H\varepsilon_{i0} \tag{16}$$

So, we introduce a nonlocal constitutive law in the form

$$\sigma_i = \tilde{A}_{ij}\varepsilon_i + \int_0^{\bar{\varepsilon}_i}\tilde{A}'_{ij}(\varepsilon_i, A, \lambda)\alpha(\varepsilon_i, A, \lambda)d\varepsilon_i \tag{17}$$

i =1,2…6, where the nonlocal functions A'_{ij} and the weighting function α are unknown.

Now our identification problem can be formulated in the following.

Given P pairs experimental values $\sigma_k^{\exp}$, $\varepsilon_k^{\exp}$, k=1,… P find the functions $\tilde{A}'_{ij}(\varepsilon, A, \lambda)$ and α such that the functional

$$E(\tilde{A}', \alpha) = \sum_{k=1}^{P}\int_0^{L_k}(\sigma_k - \sigma_k^{\exp})^2 dp = \sum_{k=1}^{P} e_k^2 \tag{18}$$

is minimum, where $p=\{A, \lambda, h\}$, $A \in [0, 0.5]$, $\lambda \in [1\text{ nm}, 8\text{ nm}]$ and $h \in [0.5\,\mu\text{m}, 3\,\mu\text{m}]$ and e_k the residuals. We choose for $\tilde{A}'_{ij}(\varepsilon, A, \lambda, h)$ the following form

$$\tilde{A}'_{ij}(\varepsilon_i, A, \lambda, h) = \sum_{k=1} B_{ij}^{(k)}(A, \lambda, h) \sin N\pi\varepsilon_i \tag{19}$$

where B are estimated using the experimental data.

In this paper we use the experimental results available in [1] for composition-modulated Au-Ni and Cu-Pd foils. Tests were made on eleven Au-Ni foils having composition modulations with wavelengths ranging from 7.1 to 1.5 nm with average compositions between 50 and 65 % Ni and on six Cu-Pd foils having an average composition of 62% Pd (four specimens) and 80% Pd (two specimens). The numerical results show that a good compromise is obtained for

$$\begin{aligned}\tilde{A}'_{ij}(\varepsilon_i, A, \lambda, h) &= \frac{1}{2} B_{ij}(A, \lambda, h) \sin \pi\varepsilon_i \\ &+ C_{ij}(A, \lambda, h) \sin 2\pi\varepsilon_i\end{aligned} \tag{20}$$

and $\alpha(x)$ is a suitable empirical weighting function of the form

$$\begin{aligned}\alpha(\varepsilon_i, A, \lambda, h) &= \frac{\pi}{2}[B_{ij}(A, \lambda, h) \sin^2 \frac{\pi\varepsilon_i}{2} \\ &+ C_{ij}(A, \lambda, h) \sin^2 \pi\varepsilon_i]^{-1/2}\end{aligned} \tag{21}$$

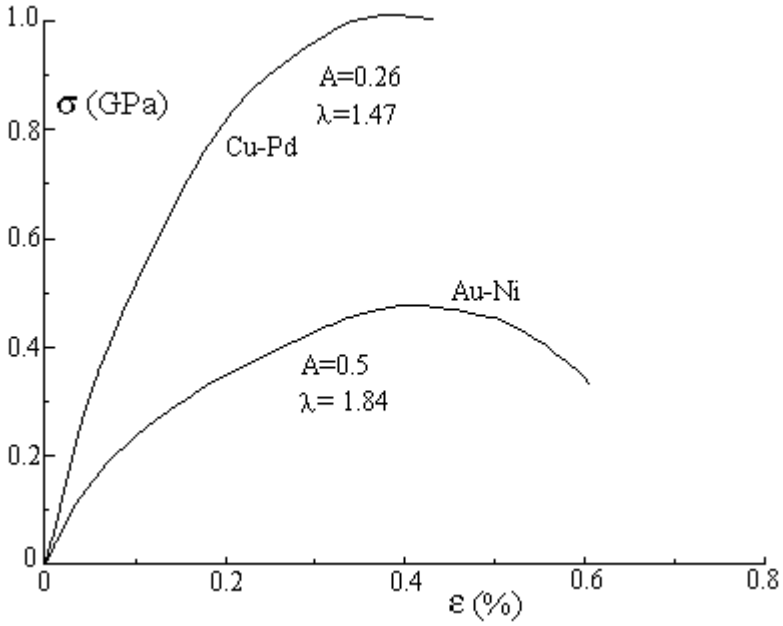

Fig.2. Theoretical stress-strain curves for a Au-Ni foil
(λ =1.84 nm , h =2.23 μ m , A=0.5) and a Cu-Pd foil (λ =1.47 nm , h =1.17 m , A=0.26).

On introducing (20) and (21) into (16) we obtain the final form of the constitutive law

$$\begin{aligned}\sigma_i &= \tilde{A}_{ij}\varepsilon_i + [B_{ij}(A, \lambda, h) \sin^2 \frac{\pi\bar{\varepsilon}_i}{2} \\ &+ C_{ij}(A, \lambda, h) \sin^2 \pi\bar{\varepsilon}_i]^{1/2}\end{aligned} \tag{22}$$

In (21) we have 9+9 unknown functions B_{ij} and C_{ij} . The optimization algorithm uses the Newton-Raphson numerical method. The numerical results of identification show a good agreement between model and experiment. The results have shown that the nonlinearity increases with

increasing amplitude of the composition modulation.

It is a routine matter now to compute the stress field induced by the strain input ε. Fig. 2 shows the constitutive stress-strain curves for the Au-Ni foil (λ = 1.84 nm , h = 2.23 μm , A= 0.5).In the case of this wavelength, a higher initial slope than the curves for longer wavelengths is obtained in agreement with the experimental results. Fig.2 also shows the constitutive curve for the Cu-Pd foil (λ = 1.47 nm, h = 1.17 μm, A = 0.26). In this case, for short-wavelength specimen (1.47 nm) a substantial increase in the initial slope is observed with increasing amplitude of the composition modulation, in agreement with the experimental results.

3. THE INVERSE PROBLEM

The evaluation of the elastic moduli is performed from the wave velocities v_i , i = 1,2… P data obtained in the direct problem. We have not the experimental values, so we have been multiplied v_i by $(1+r_i)$ with r_i three random numbers uniformly distributed in the interval $[-q,q]$ where $q = 10^{-3}, 10^{-2}, 10^{-1}$.

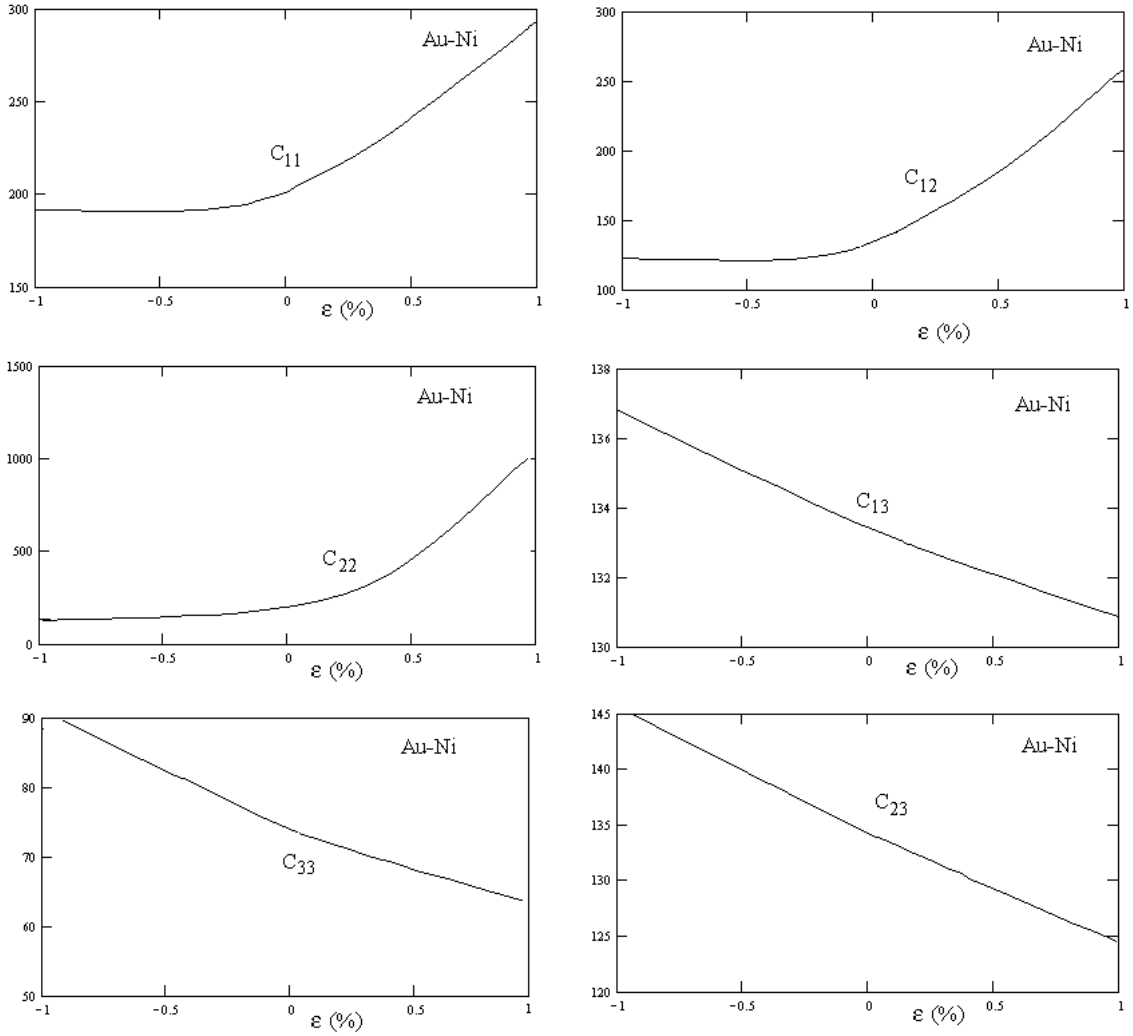

Fig.3. Variation of the elastic constants $C_{11}, C_{12}, C_{13}, C_{22}, C_{23}$ with the initial strain ε for Au-Ni.

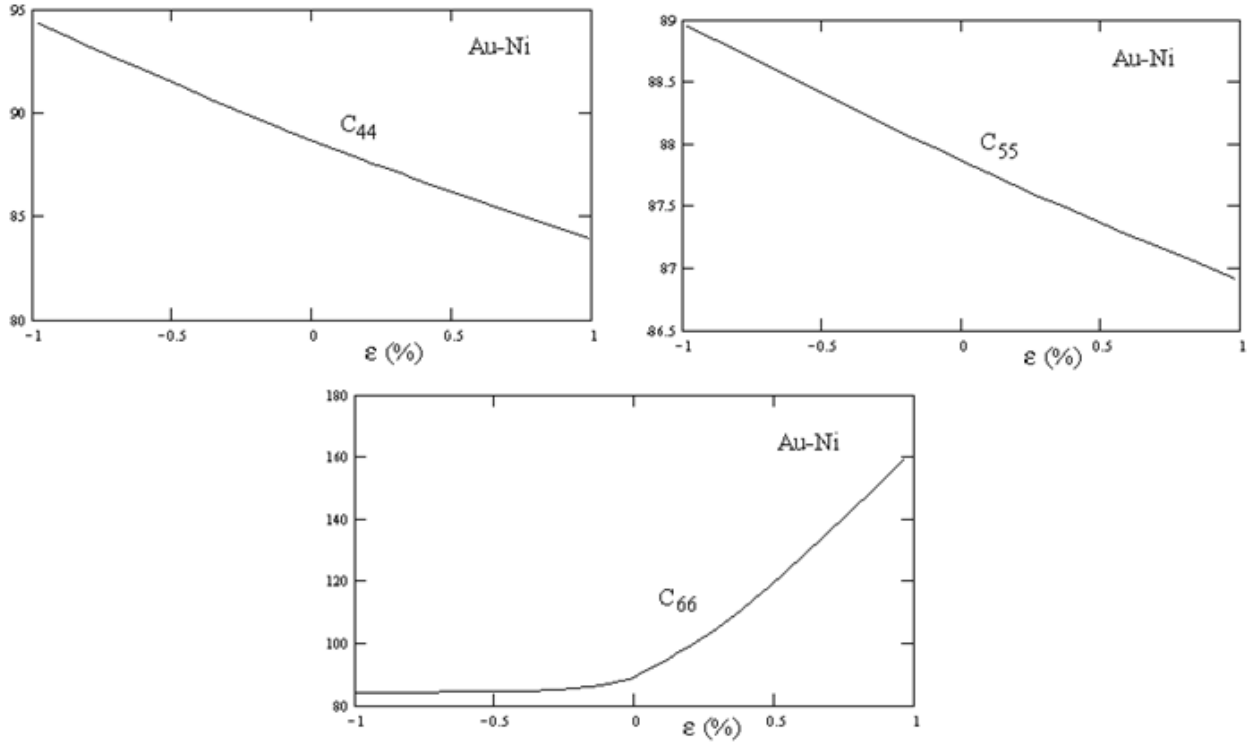

Fig. 4. Variation of the elastic constants C_{44}, C_{55}, C_{66} with the initial strain ε for Au-Ni.

The effect of the initial strain on the elastic constants is different. The values of constants increase with negative deformations and C_{11}, C_{22}, C_{12}, C_{66} increase with positive deformations. The variation of the elastic constants with the initial strain ε are given in Fig.3 and Fig.4 for Au-Ni. The calculations were made for $\lambda = 1.8$ nm, A=0.5 in the case of the Au-Ni foil, and $\lambda = 1.5$ nm, A=0.26 for Cu-Pd.

The biaxial modulus Y[111] is calculated as the initial slope in the constitutive curve stress-strain. The biaxial modulus is increasing for negative deformations in both cases (Fig. 5). The biaxial modulus decreases with increasing strain for $\varepsilon \le 0.5$ in the case of Au- Ni foils, and for $\varepsilon \le 0.1$ in the case of Cu-Pd. For $\varepsilon > 0.5$ (Au-Ni) and $\varepsilon > 0.1$ (Cu-Pd) the modulus increases with increasing strain.

The variation of Y[111] with wavelength λ for Au-Ni and respectively, for Cu-Pd are shown in fig.6 for $\varepsilon = -0.1$. For approximately λ=1.8 nm, in the case of a Au-Ni, and λ=1.5 nm, in the case of a Cu-Pd foil, the biaxial modulus is maximum.

The numerical evaluations of the inverse problem behave well with respect to measurement noise. The convergence and accuracy remain good in all cases. The determination of elastic constants and therefore, of the biaxial modulus appear to be not very sensitive to data noise. Values of the elastic constants and biaxial modulus (GPa) as a function of the initial strain ε (%) for Au-Ni are presented in Table 1, and the values of the elastic constants and biaxial modulus (GPa) as a function of the initial strain ε (%) for Cu-Pd are presented in Table 2.

Table 1. Values of the elastic constants and biaxial modulus (GPa) as a function of the initial strain ε (%) for Au-Ni

ε	C_{11}	C_{12}	C_{13}	C_{22}	C_{23}	C_{33}	C_{44}	C_{55}	C_{66}	Y[111]
-1	193.00	123.00	136.25	135.00	144.77	880.43	93.64	88.88	82.00	814.06
-0.9	193.14	123.15	135.97	135.48	143.72	806.78	93.16	88.78	82.13	806.48
-0.8	193.38	123.44	135.68	136.82	142.66	768.90	92.63	88.67	82.34	797.21
-0.7	193.72	123.87	135.40	139.12	141.61	730.11	92.12	88.57	82.64	779.16
-0.6	194.19	124.48	135.11	142.54	140.55	609.34	91.61	88.47	83.05	750.54

-0.5	194.80	125.27	134.83	147.25	139.49	360.45	91.10	88.36	83.57	710.46
-0.4	195.58	126.30	134.54	153.46	138.44	236.55	90.59	88.26	84.22	659.61
-0.3	196.56	127.59	134.26	168.43	137.38	168.50	90.04	88.16	85.04	600.69
-0.2	197.76	129.20	133.97	171.15	136.33	128.55	89.57	88.05	86.05	538.26
-0.1	199.25	131.18	133.69	184.10	135.27	103.98	89.06	87.95	87.29	477.64
0	201.08	133.63	133.40	199.70	134.22	88.37	88.55	87.85	88.80	423.69
0.1	203.32	136.65	133.12	219.15	133.16	78.21	88.04	87.74	90.63	379.72
0.2	206.09	140.38	132.83	243.24	132.11	71.50	87.53	87.64	92.94	347.24
0.3	209.52	145.01	132.55	273.31	131.05	67.03	87.02	87.54	95.77	326.31
0.4	213.81	150.81	132.26	311.12	130.00	64.06	86.51	87.43	99.31	316.17
0.5	219.25	158.18	131.98	359.26	128.94	62.10	86.00	87.33	103.78	315.91
0.6	226.26	167.68	131.69	421.57	127.89	60.82	85.50	87.23	109.55	324.93
0.7	235.52	180.25	131.41	504.10	126.83	60.02	84.99	87.13	117.15	343.40
0.8	248.14	197.38	131.12	616.87	125.78	59.54	84.48	87.02	127.55	372.80
0.9	266.12	221.81	130.84	778.90	124.72	59.27	83.97	86.92	142.27	416.95
1	293.44	258.96	130.55	1023.0	123.66	59.18	83.46	86.82	164.68	484.57

Table 2. Values of the elastic constants and biaxial modulus (GPa) as a function of the initial strain ε (%) for Cu-Pd

ε	C_{11}	C_{12}	C_{13}	C_{22}	C_{23}	C_{33}	C_{44}	C_{55}	C_{66}	Y[111]
-1	162	104	128.36	114.03	121.03	510.44	79.40	75.13	69	474.34
-0.9	162.13	104.15	114.51	114.43	120.34	505.22	78.99	75.06	69.13	467.92
-0.8	162.35	104.40	114.29	115.58	119.48	495.12	78.58	74.99	69.32	460.50
-0.7	162.66	104.78	114.07	117.55	118.62	488.13	78.17	74.92	69.59	447.21
-0.6	163.07	105.31	113.85	120.47	117.76	05.99	77.75	74.85	69.95	428.86
-0.5	163.60	105.99	113.63	124.48	116.90	397.24	77.34	74.78	70.41	407.65
-0.4	164.28	106.87	113.41	129.76	116.05	293.26	76.93	74.71	70.98	386.41
-0.3	165.12	107.98	113.19	136.54	115.19	236.11	76.51	74.63	71.7	367.61
-0.2	166.16	109.35	112.97	145.08	114.33	202.54	76.10	74.56	72.57	352.72
-0.1	167.44	111.03	112.75	155.75	113.47	181.88	75.69	74.49	73.64	342.23
0	169	113.11	112.53	169	112.61	168.74	75.27	74.42	74.94	335.95
0.1	170.91	115.65	112.31	185.39	111.75	160.18	74.86	74.35	76.53	333.45
0.2	173.25	118,79	112.09	205.72	110.89	154.53	74.45	74.28	78.48	334.29
0.3	176.16	122.68	111.87	231.04	110.03	150.76	74.03	74.21	80.89	338.17
0.4	179.77	127.54	111.65	262.81	109.17	148.26	73.62	74.14	83.89	345.01
0.5	184.35	133.68	111.43	303.15	108.31	146.60	73.21	74.07	87.68	354.99
0.6	190.22	141.58	111.21	355.19	107.45	145.53	72.79	74	92.53	368.69
0.7	197.93	151.98	110.99	423.83	106.59	144.85	72.38	73.92	98.91	387.18
0.8	208.39	166.87	110.77	517.11	105.73	144.45	71.97	73.85	107.54	412.43
0.9	223.16	186.02	110.55	649.29	104.87	144.24	71.56	73.78	119.74	448.06
1	245.36	215.99	110.33	848.29	104.01	144.16	71.14	73.71	138.05	501.30

4. CONCLUSIONS

The paper is concerned with small amplitude oscillations in initially deformed elastic metallic bilayers. The variation of sound speeds with initial strain and the measured magnitude of the acousto-elastic effect are used to determine the biaxial modulus and the elastic constants for a deformation in the [111] direction. Our numerical results shown that the foils containing short-wavelength compositions modulations has an enhanced biaxial modulus Y[111] both for Au-Ni and Cu-Pd.

The deformation is non-Hookian – the biaxial modulus given by the slope of the stress-strain curves decreases with increasing strain for Au- Ni. For Cu-Pd the modulus decreases with increasing strain for $\varepsilon \leq 0.7\%$ and for $\varepsilon > 0.7$ % it increases with increasing strain. As compared with homogeneous foils at the same average compositions, the modulated foils exhibit an appreciable increase in modulus Y[111] as a function of ε. For example, the modulus increases from 423 GPa ($\varepsilon = 0\%$) to 477 GPa ($\varepsilon = -0.1\%$) , 710 GPa ($\varepsilon = -0.5\%$) for Au-Ni, and from 335 GPa ($\varepsilon = 0\%$) to 342 GPa ($\varepsilon = -0.1\%$),

407 GPa (ε = -0.5%) for Cu-Pd.The results are consistent with the experimental results obtained by Yang, Tsakalakos and Hilliard in 1977.

REFERENCES

1. YANG, W. M. C., TSAKALAKOS, T., HILLIARD, J.E., *Enhanced elastic modulus in composition-modulated gold-nickel and copper-palladium foils*, J. Appl. Phys., 48, 876-879, 1977.
2. DELSANTO, P.P., PROVENZANO, V., UBERALL, H., *Coherency strain effects in metalic bilayers*, J. Phys.: Condens. Matter, 4, 3915-3928, 1992.
3. JANKOWSKI, A.F., TSAKALAKOS, T., *The effect of strain on the elastic constants of noble metals*, J. Phys. F: Met. Phys., 15, 1279-1292, 1985.
4. JANKOWSKI, A.F., *Modelling the supermodulus effect in metallic multilayers,* J. Phys. F: Met. Phys., 8, 413-427, 1988.
5. BARAL, D., HILLIARD, J.E., JETTERSON, J.B., MIYANO, K., *Determination of the primary elastic constants from thin foils having a strong texture*, J. Appl., Phys., 53, 5, 1982.
6. TSAKALAKOS, T., HILLIARD, J.E., *Elastic modulus in composition-modulated copper-nickel foils*, J. Appl. Phys., 54(2), 734-737, 1983.
7. CHIROIU, V., DELSANTO, P.P., MUNTEANU, L., RUGINA, C., SCALERANDI, M., *Determination of the second- and third-order elastic constants an Al from the natural frequencies*, J. Acoust. Soc. Am., 102(1), 1997.
8. NEDELCU, N.,CHIROIU, V., RUGINĂ, C., MUNTEANU, L., IOAN, R., GIRIP, I., DRAGNE,C., *Preparation of GeSbSe thin films by conventional melt-quenching method and studying their characteristics*, Results in Physics, vol 16, Martie 2020, paper 102856, 2211-3797, 2020.
9. NEDELCU, N., CHIROIU, V., RUGINĂ, C., MUNTEANU, L., IOAN, R., GIRIP, I., DRAGNE, C., *Dielectric properties of GeSbSe glasses prepared by the conventional melt-quenching method,* Results in Physics, 16, paper 102856, 2020.
10. NEDELCU, N., CHIROIU, V., MUNTEANU, L., GIRIP, I., *On the optical nonlinearity in the GeSbSe chalcogenide glasses*, Materials Research Express, 7(6), 1-15, 2020.
11. NEDELCU, N., CHIROIU, V., MUNTEANU, L., GIRIP, I., *Characterization of GeSbSe thin films synthesized by the conventional melt-quenching method,* Spectroscopy-IR Spectroscopy for today's Spectroscopists, 22-33, vol 35, S3, 2020.
12. CHIROIU, Călin, *An unified theory of evolution and structure of matter*, Modelling, Measurement & Control, A , AMSE Press, 51(3), 19-26, 1993.
13. CHIROIU, Călin, CHIROIU, V., SCALERANDI, M., *Modelling the Supermodulus Effect in Metallic Modulated Structure,* SISOM 98, 1998.
14. CHIROIU, Călin, *Ultrasound waves in initial deformed elastic metallic bilayers, part I* : *Theoretical Model*, Rev. Roum. Sci. Techn, 43(6), 1998.
15. CHIROIU, Călin, *Ultrasound waves in initial deformed elastic metallic bilayers, part II* : *Numerical Simulations*, Rev. Roum. Sci. Techn, 44 (2), 1999.
16. SCALERANDI, M., DELSANTO, P.P., CHIROIU, C., CHIROIU, V., *Numerical simulation of pulse propagation in nonlinear 1-D media,* Journal of the Acoustical Society of America, 106, 2424-2430, 1999.
17. IOAN, R., MUNTEANU, L., DUMITRIU, D., *Determination of Dynamic Young's Modulus for Steel Alloys,* Romanian Journal of Mechanics, 1(1), 3-12, 2016.
18. KRONER, E., *Elasticity theory of materials with long range cohesive forces*, Int. J. Solids and Structures, 3, 731-742, 1967.
19. ERINGEN, A. C., *Linear theory of nonlocal elasticity and dispersion of plane waves*, Int. J. Engng Sci, 10, 425-435, 1972.
20. ERINGEN, A. C., *On differential equations of nonlocal elasticity and solutions of screw dislocations and surface waves*, J. Appl. Phys. 54, 4703-4710, 1983.

Received June 21, 2020